Received January 13, 2021, accepted January 25, 2021, date of publication February 4, 2021, date of current version February 17, 2021.

Digital Object Identifier 10.1109/ACCESS.2021.3057292

Cooperative Spectrum Prediction-Driven Sensing for Energy Constrained Cognitive Radio Networks

PRAKASH CHAUHAN[1], SANJIB K. DEKA[1], (Member, IEEE), BIJOY CHAND CHATTERJEE[2], (Senior Member, IEEE), AND NITYANANDA SARMA[1], (Member, IEEE)

[1]Department of Computer Science and Engineering, Tezpur University, Tezpur 784028, India
[2]Department of Computer Science, South Asian University, New Delhi 110021, India

Corresponding author: Prakash Chauhan (prakashc@tezu.ernet.in)

ABSTRACT Spectrum prediction based sensing schemes minimize the overall energy consumption of the sensing module in cognitive radio networks (CRNs) by predicting the status of spectrum before performing actual physical sensing. But, the performance of independent or local prediction models suffer from inaccuracies. Cooperative mode of spectrum prediction is found to be suitable to overcome the issues of local prediction models. In this work, we propose a cooperative spectrum prediction-driven sensing scheme for energy constrained cognitive radio networks to reduce the energy consumption while maintaining the spectral efficiency. The proposed scheme first employs a long short term memory network technique to perform local spectrum prediction, which identifies the status of a channel before actual sensing to improve energy efficiency. Thereafter, a parallel fusion based cooperative spectrum prediction model is applied to minimize the errors induced in local prediction model. Finally, the resultant cooperative prediction model is combined with a spectrum sensing framework to perform sensing operation when the cooperative spectrum prediction results to an indeterminate state in order to enhance the spectral efficiency. Simulation results show the efficacy of the proposed scheme in terms of spectral efficiency and energy efficiency compared to similar schemes from literature.

INDEX TERMS Cognitive radio networks, energy efficiency, prediction-driven sensing, spectral efficiency, spectrum prediction.

I. INTRODUCTION

With the advancement of technology, the usage of wireless devices increases enormously from the last decades [1]. The ubiquitous uses of these wireless devices demand for large amount of radio spectrum. As most of the radio spectrum region are already being allocated to existing wireless services, there has been a spectrum scarcity problem that arises for emerging wireless services. The recent measurements carried out by Federal Communications Commission (FCC) have shown that 70% of the allocated spectrum in US is not utilized [2]. This motivates the development of the concept of cognitive radio (CR) [3], which allows CR enabled users or secondary users (SUs) to utilize the licensed radio spectrum when the spectrum is temporally not being utilized by its licensed users or primary users (PUs).

The associate editor coordinating the review of this manuscript and approving it for publication was Barbara Masini.

In today's CR networks (CRNs), SUs are mostly battery driven wireless devices and have energy constraints in terms of power [4]–[6]. In energy constrained CRNs, spending more energy in sensing would lead to less energy available for transmission, which degrades the overall spectrum utilization. In such energy constrained CRNs, energy efficiency (EE) and spectral efficiency (SE) become two important aspects that need due attention to make communication viable. SE implies efficient utilization of spectrum holes, whereas, EE states minimal energy depletion for achieving desired level of SE.

Spectrum sensing is a key functionality to detect the presence of PUs in licensed channels but it incurs considerable energy overhead. In high traffic CRNs [7], the possibility of licensed channels being busy is very high. Thus, a random selection of channels for sensing incurs high energy overhead as well as increases waiting time of SUs, which eventually reduces the transmission time. Spectrum prediction or channel state prediction based sensing schemes [8] select only

This work is licensed under a Creative Commons Attribution 4.0 License. For more information, see https://creativecommons.org/licenses/by/4.0/

those channels for sensing that are likely to be idle in the next successive slots. Thus, usage of spectrum prediction method along with sensing framework reduces the overall waiting time of SUs to find idle channel for transmission, and eventually enhances spectral efficiency. Although prediction module requires additional time but it can be compensated to overall time spent by SUs for sensing, which includes time to decide when and what channels to be sensed to find free slots for data transmission. Further, spectrum prediction based sensing reduces the overall energy consumption during spectrum sensing, and thereby improves energy efficiency of SUs.

Spectrum prediction schemes [8]–[10] typically use machine learning (ML) techniques to locally predict the future channel availability using the spectrum sensing history. The work in [8] discusses multilayer perceptron (MLP) based channel status prediction model, which can explore the spectrum holes based on the past sensing history and selects the channel predicted to be idle. In [9], a hidden markov model (HMM) based channel state prediction scheme is presented, which minimizes the delay that gets incurred during real-time spectrum sensing by performing spectrum prediction. Another, HMM based spectrum prediction method is discussed in [10], which represents the spectrum prediction as a pattern classification problem and considers higher number of hidden states to capture the different levels of PU's activity, hence increasing the span of prediction very unlikely in the traditional HMM based spectrum prediction model. To perform spectrum prediction in energy-constrained CRNs, a HMM based prediction technique is presented in [11] which classified the SUs into two sets namely Interfered by PU (IP) and Non-interfered by PU (NIP). The SUs that are interfered by PUs are prevented from spectrum sensing to save energy consumption. In CRNs under Global System for Mobile Communications (GSM) based primary networks [12], SUs that are located closer to PU are not allowed to access the licensed channel as SU transmissions in this situation may cause interference to PU. A support vector machine (SVM) based spectrum prediction technique is discussed in [13], which enhances the energy-efficiency of the CRN by optimizing prediction duration and prediction energy under network different environments.

The works in [14], [15] discuss long-term spectrum state prediction techniques which are found to be better for dynamic spectrum access (DSA) in comparison to short-term prediction in CRNs. In short-term prediction, spectrum prediction is performed for single time slot in a slot by slot manner whereas long-term prediction aims to get status of multiple time slots at any particular time, which eventually improves the accessibility of the vacant spectrum. Authors in [14], [15] use tensor based model to obtain the long-term status of spectrum in different dimensions such as time, frequency, and day. Another work which emphasizes the significance of machine learning in prediction to perform DSA for next generation networks like CR enabled internet of things (IoTs) is discussed in [16]. The work discusses the state-of-the-art ML techniques employed in DSA, a structured taxonomy of DSA via ML, challenges, and open issues for future directions.

However, local prediction [8]–[10] results usually suffer from inaccuracy due to possible learning error and data errors likely to be present in historical sensing dataset collected through independent sensing. The errors in dataset are mainly due to the erroneous environment. To overcome the issues of local spectrum prediction, cooperative mode of spectrum prediction are presented in [7], [17]–[19], which leverage a collaborative decision about PU existence through the fusion of the local prediction results of geographically distributed secondary users (SUs). The work in [17], [18], presents collaborative approaches for spectrum prediction under various PU traffic conditions to minimize error probability that may incur during local spectrum prediction in term of PU's activity pattern and the sensing error. The work in [7] presents a cooperative spectrum prediction model (CPM), which makes use of past sensing data. Their model uses MLP and HMM for prediction and performs spectrum sensing for only those channels that are predicted to be available. Although the authors in [7] claim to reduce energy consumption for sensing, SE is also reduced due to false prediction. A cooperative prediction-and-sensing based spectrum sharing (CPSS) model presented in [19] performs spectrum sensing for all channels irrespective of spectrum prediction results. This leads to improved detection accuracy, and hence higher SE, but at the expense of increased energy overhead. It performs sensing to all channels irrespective of the output of spectrum prediction operation.

Due to usage of MLP based prediction [7], [8], [19], these models cannot handle sequence dependence issues of time series prediction problems. The HMM based prediction model [9], [10], [18] has a very high complexity while predicting large number of future slots. Furthermore, the cooperation based prediction models [7], [19], which resolve the issues of local spectrum prediction problem typically use fixed value of κ in κ-out-of-N fusion rule during fusion. Due to the fixed value of κ, it may not be able to capture the fluctuations in received primary user (PU) signal, which arises due to environmental noise and fading effects [20].

To handle the sequence dependency issues, which arise in MLP based time series spectrum prediction model and to predict status of a large number of future spectrum slots, a long short term memory (LSTM) network based spectrum prediction is presented in [21]. The work in [21] uses LSTM to predict the power spectral density (PSD) values of a channels and applies taguchi method for network structure optimization of local prediction model. However, the work in [21] only discusses the local mode of spectrum prediction problem and lacks in capturing the error scenarios, which arise during local spectrum prediction. Since, the foundation of cooperation based prediction scheme for CRNs envisions to reduce the overall energy consumption during spectrum opportunity detection while maintaining a high spectrum utilization, development of an efficient cooperation based prediction scheme is highly desirable, which can reduce the energy consumption during sensing while maintaining a higher SE. The cooperation based prediction model should also handle the sequence dependency issues and incorporate the adaptability of fusion rule that captures the network environment variations.

The main objective of this article is to develop a cooperative spectrum prediction-driven sensing scheme for energy constrained CRNs, which reduces the energy consumption while maintaining SE during spectrum opportunity detection. A cooperative prediction-driven sensing adopted in the proposed scheme helps in enhancing both detection accuracy and energy efficiency. The overall contributions of this article are summarized as follows:

- We employ an LSTM network based local prediction model for two aspects - (a) to identify the status of a channel before performing the actual sensing in order to improve EE and (b) to handle the sequence dependency issues in time series prediction problems that exist in MLP based prediction model [7], [19].
- We apply the results from local prediction model to a parallel fusion based cooperative prediction model to reduce the local prediction errors that may exist in the independent prediction model like in [21] and capture the network environment variations through a dynamically configurable value of κ in κ-out-of-N fusion rule.
- The resultant cooperative prediction model is combined with a spectrum sensing framework to perform sensing operation when the cooperative spectrum prediction results in an indeterminate state in order to enhance detection accuracy, which eventually increases SE.
- Simulation based evaluation of the proposed scheme is carried out to show the efficacy of the proposed scheme in terms of SE and EE compared to similar schemes from literature. Simulation results also reveal that incorporating an adaptive κ-out-of-N fusion rule in the proposed scheme leads to better performance than the conventional majority-fusion rule used in [7], [19] at higher error levels in time series data.

The rest of this article is organized as follows. Section II discusses the system model and assumptions. In Section III, the proposed scheme is presented. The performance evaluation of the proposed scheme with the existing schemes is discussed in Section IV followed by the conclusion in Section V.

II. SYSTEM MODEL AND ASSUMPTIONS

A centralized network architecture is assumed, which consists of a set of N number of SUs denoted by $\mathcal{N} = \{1, 2, \ldots, N\}$, a set of M number of PU channels denoted by $\mathcal{M} = \{1, 2, \ldots, M\}$, and a fusion center (FC). It is assumed that SUs are battery enabled and have energy constrained in terms of power. Further, it is assumed that PUs fall under the sensing range of SUs and FC. Also, FC located at central position with respect to SUs and acts as a central entity for SUs, which is given the responsibility of performing cooperative prediction activities and spectrum sensing when the result of cooperative prediction is found to be indecisive. This leads to reduction in spectrum sensing overhead of SUs. A diagram of the assumed network architecture is shown in Fig. 1. FC performs spectrum sensing using energy detection (ED) [22]. To synchronize SUs with PU, a time-slotted system is considered as in [23], [24] and SUs access the channel in a time division multiple access (TDMA) fashion. Each time slot (T) is further divided into three sub-slots, named as prediction time (t_p), sensing time (t_s), and transmission time (t_t) respectively. All the information between SUs and FC are communicated using a dedicated common control channel [20].

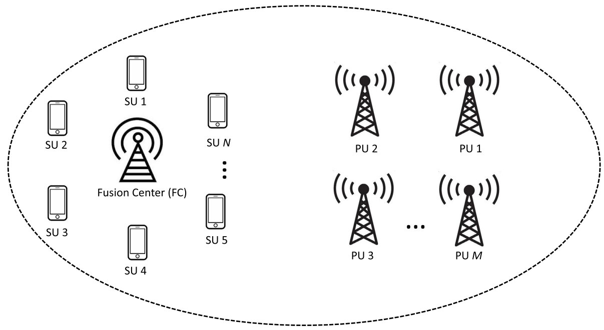

FIGURE 1. Network architecture.

We model spectrum prediction as a time-series prediction problem [8], where the binary time series data have been prepared from sensing history of PU channels. The binary time series for a channel is prepared by employing ED over channels for Z slots, where $\mathcal{Z} = \{1, 2, \ldots, Z\}$ and the estimated strength of the received signal, $Y(z)$, at time slot z, $\forall z \in \mathcal{Z}$ is then compared with the sensing threshold λ_s to decide on the status of a channel. For SU $n \in \mathcal{N}$, at a given time slot $z \in \mathcal{Z}$ of channel $m \in \mathcal{M}$, the sensing status of the channel, $\Omega^n_{m,z}$, is given by (1).

$$\Omega^n_{m,z} = \begin{cases} 0, & \text{if } Y(z) < \lambda_s, \\ 1, & \text{Otherwise} \end{cases} \tag{1}$$

where $\Omega^n_{m,z}$ equals to 0 or 1, respectively, indicate the absence and presence of PU activity.

Every SU prepares a time series for each channel based on their own sensing. λ_s can be decided empirically [25] or as given in [26]. It is considered that before the starting of the prediction module, SUs perform spectrum sensing independently over PU channels for a large number of slots in order to collect sufficient sensing data for prediction. Once a SU starts its prediction module and observes that it's prediction accuracy falls below a designated threshold compared to the final cooperative result, the SU immediately stops its prediction module and restarts sensing module to collect new set of sensing data in order to improve its prediction.

The noise environment is assumed to be circularly symmetric complex gaussian (CSCG) and each PU uses complex-valued phase shift keying (PSK) signals for data transmission [27]. The two metrics which determine the

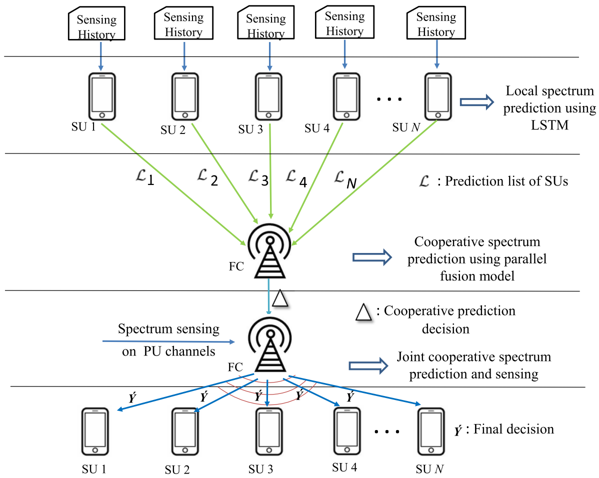

FIGURE 2. Different phases of the proposed scheme.

performance of a spectrum sensing, namely the probability of detection (P_d) and the probability of false alarm (P_f). The P_d indicates the probability of correctly detecting the PU signal when it is actually present, and P_f indicates the probability of falsely detecting the PU signal when it is actually absent. The probability of false alarm and probability of detection for each SU are computed using (2) and (3) [27], respectively.

$$P_f = Q\Big(\big(\frac{\lambda_s}{\sigma^2} - 1\big)\sqrt{t_s f_s}\Big) \tag{2}$$

$$P_d = Q\Big(\big(\frac{\lambda_s}{\sigma^2} - \gamma - 1\big)\sqrt{\frac{t_s f_s}{2\gamma + 1}}\Big) \tag{3}$$

where, σ^2 represents noise variance, γ refers to signal-to-noise ratio, $Q(.)$ indicates complementary distribution function, and f_s sampling frequency. Since, the probability of miss detection (P_m) is complement of the probability of detection and it can be given by (4).

$$P_m = 1 - P_d \tag{4}$$

III. PROPOSED SCHEME

The proposed scheme comprises of three phases: local spectrum prediction, cooperative spectrum prediction, and joint prediction and sensing. In local spectrum prediction phase, every SU performs local prediction based on their sensing history and sends their prediction results to FC. In the cooperative prediction phase, FC performs cooperation on local prediction results received from SUs to achieve a cooperative decision about the existence of PU. In the joint prediction and sensing phase, FC performs spectrum sensing using the ED framework to decide the status of those slots of channels could not be predicted with certainty by cooperative prediction. A diagrammatic representation of different phases of the proposed scheme is shown in Fig. 2.

A. LOCAL SPECTRUM PREDICTION

In this phase, we employ an LSTM network [21], which handles long term dependencies in time series data at each SU to perform spectrum prediction. LSTM networks are basically made up of memory blocks that are inter-connected through layers of neurons. The main components of memory blocks are cells and gates, where cells are primarily used to store the temporal state information and gates are used to regulate the in/out-flow of information to/from the memory cells. A basic block diagram of LSTM is given in Fig. 3. The cell and hidden state are being propagated to the next cell and information about the gradients are stored in the memory blocks. The contents of the memory block is manipulated with the help of some structural unit, called gates.

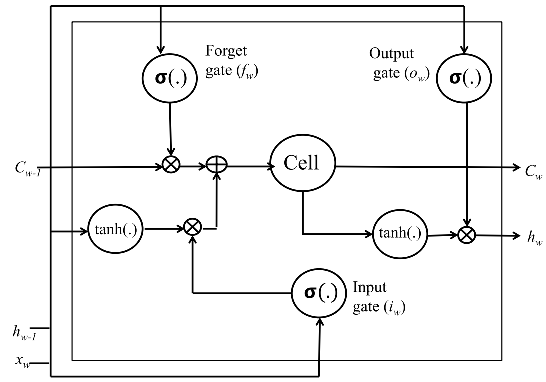

FIGURE 3. A block diagram of long short-term memory.

There are basically three gates available in a LSTM unit: input, output, and forget gates. The input gate decides about which input flows into the memory cell, the output gate controls the outflow of cell information to the network and the forget gate is responsible for resetting of cell's memory. As shown in the Fig. 3, (i_t), (o_t) and (f_t) represent input, output and forget gate, respectively. $\sigma(.)$, tanh(.), $\bigoplus$, and $\bigotimes$ represent sigmoid activation function, hyperbolic tangent activation function, addition and multiplication, respectively. In order to determine the value of cell state (c_t) and hidden state (h_t) based on an input variable (x_t) at a particular instance (t), a set of computations are involved in feed forward propagation that can be discussed in the form of equations as follows [28]:

$$f_t = \sigma(w_f h_{t-1} + w_f x_t + b_f) \tag{5}$$

$$i_t = \sigma(w_i h_{t-1} + w_i x_t + b_i) \tag{6}$$

$$l_t = \tanh(w_c h_{t-1} + w_c x_t + b_c) \tag{7}$$

$$c_t = f_t \odot c_{t-1} + i_t \odot l_t \tag{8}$$

$$o_t = \sigma(w_o h_{t-1} + w_o x_t + b_o) \tag{9}$$

$$h_t = o \odot \tanh c_t \tag{10}$$

where, the w's and b's terms indicate different weight matrices and bias vectors to different gates, respectively, and $\odot$ represent element-wise multiplication operation. The time series data for any channel is divided into two parts: training data and testing data. The training data are fed into the LSTM network based local spectrum prediction (LSP) model as input during the training phase. The training is continued until the error, which can be determined using mean squared error (MSE), is brought down to a desired level or maximum number of epochs (ξ) set is reached. Once the training is over, testing is performed using the testing data.

In LSP, an iterative approach is adopted to tune the hyper parameters of LSTM network to achieve a desired level of accuracy in prediction. To start with, each of the hyper-parameter is assigned a range of values. Whichever combination of values of the parameters gives better training accuracy, that combination is considered to be the final values of those parameters. For cross-validation of LSP, a basic model of nested cross-validation [29] is employed since the traditional cross-validation techniques are not suitable for time-series data due to its temporal dependencies. Using LSP, every SU prepares a prediction list, which contains local prediction results for a set of L future slots denoted by $\mathcal{L} = \{1, 2, \ldots, L\}$, for each of the M channels, and sends the prediction lists to FC using a common control channel. Since an exhaustive search on all combinations of all possible values of hyper parameters has not been done, this iterative approach does not claim the optimal tuning of hyper-parameters for LSP model.

B. COOPERATIVE SPECTRUM PREDICTION

In this phase, we introduce a cooperative spectrum prediction (CSP) model. The cooperative prediction model for collaboration is harnessed by incorporating learning error, α_e and sensing data error, β_e. Here, α_e indicates the errors generated by the prediction model when a particular learning algorithm in the model uses error-free dataset, whereas β_e indicates the errors that exist in the sensing dataset collected from spectrum sensing operation.

In network environment variations, where environmental noise and fading effects get changed spatio-temporarily, β_e also varies according to the network environment. This is because, while SUs perform sensing using ED, the fluctuations in SNR affects overall sensing [30] and deteriorates the performance when SNR level reaches to a significantly low value. Due to the deteriorated sensing performance, more errors are introduced in the sensing dataset and as a result β_e increases. To capture such dynamics in network environment, we introduce an adaptive κ-out-of-N fusion rule (AF), which dynamically determines κ, that is, the number of SUs that take a cooperative decision at a particular time slot for a channel. As the value of α_e or β_e increases, it triggers a larger value for κ (that is, considers more number of SUs for cooperation) to compensate for the local prediction errors of SUs, whose sensing data are highly affected by environmental hazards. Again, when the value of α_e or β_e becomes small, a smaller κ value is sufficient enough to take a cooperative decision over local prediction results. Considering these facts, the value of κ is determined based on the values of α_e and β_e such that it captures the changes in the network environment and is given by (11),

$$\kappa = \lceil (1 - (1 - P_{\alpha_e})(1 - P_{\beta_e}))N + 1 \rceil \tag{11}$$

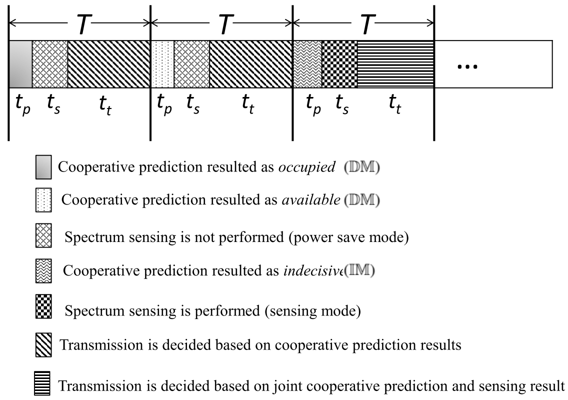

FIGURE 4. Time slot structure for the proposed scheme.

where, P_{α_e} and P_{β_e} represent probabilities of learning error and errors exist in sensing data, respectively.

We design a centralized cooperative spectrum prediction model by adopting the parallel fusion framework [31]. The cooperative spectrum prediction is implemented in the FC (or base station) only. We assign all the cooperation activities to the FC so that the SUs need to synchronize only with the FC for all cooperation activities. In the scenarios where there can be more than one FCs in the same network, cooperative spectrum prediction in the FCs can be implemented in a distributed fashion with resultant final prediction obtained through a consensus. The presence of multiple FC will increase deployment cost, message overhead as well as time required for synchronization. In ad-hoc secondary network setup, the SUs can themselves play the role of FCs and distributed cooperative spectrum sensing [32] will best suit for this purpose but at the expense of message overhead, time, and extra energy at the SUs.

While fusing the local prediction results, the cooperative model outputs two possible decision states, viz. determinate ($\mathbb{DM}$) and indeterminate ($\mathbb{IM}$). In $\mathbb{DM}$, status of a channel m at any time slot l, $\forall m \in \mathcal{M}, \forall l \in \mathcal{L}$ can either be 1 (*occupied*) or 0 (*available*). The $\mathbb{IM}$ state means, a binary decision cannot be made about the status of a channel solely on the basis of cooperative prediction, and therefore, the status of the channel is considered as -1 (*indecisive*). The *available* status indicates that PU is absent at the particular slot of the channel with certainty. In this case, SUs do not perform spectrum sensing operations and go to the power saving mode to conserve energy for the entire sensing slot (t_s). Once the sensing slot time is over, SUs can start transmission at the beginning of t_t. Similarly, when channel status is *occupied*, neither sensing nor transmission is performed for the entire slot. SUs get to the sensing mode and perform spectrum sensing to actually determine the PU's occupancy on the channel at a particular slot, when cooperative prediction outputs an $\mathbb{IM}$ state. The time slot structure for the proposed scheme is illustrated with the help of a diagram as shown in the Fig. 4.

Let N_0 and N_1 represent the number of SUs who have reported with decisions 0 and 1, respectively, to FC based on their local prediction about a time slot l of channel m.

The cooperative spectrum prediction decision at time slot l for channel m is expressed by (12),

$$\Delta_{m,l}^{d} = \begin{cases} \left.\begin{array}{ll} 0, & (N_0 \geq \kappa)\ \&\ (N_1 < \kappa) \\ 1, & (N_1 \geq \kappa)\ \&\ (N_0 < \kappa) \end{array}\right\} \mathbb{DM} \\ -1, \quad \text{otherwise} \quad \} \mathbb{IM} \end{cases} \tag{12}$$

where, $\Delta_{m,l}^{d}$ represents the cooperative spectrum prediction decision for lth time slot of channel m and & indicates the logical AND operation. Let $x_{m,l}$ be a binary variable whose value is 1 if $\Delta_{m,l}^{d} = -1$ otherwise 0 for channel m at time slot l. The probability of occurrence of indeterminate state ($P_{\mathbb{IM}}$) is estimated empirically from the prediction history of M channels over L time slots using (13).

$$P_{\mathbb{IM}} = \frac{\sum_{m=1}^{M}\sum_{l=1}^{L} x_{m,l}}{LM}, \quad \forall m \in \mathcal{M},\ \forall l \in \mathcal{L} \tag{13}$$

Therefore, the probability of occurrence of determinate state ($P_{\mathbb{DM}}$) is obtained as $P_{\mathbb{DM}} = 1 - P_{\mathbb{IM}}$.

Let P_{fp} and P_{mp} represent the probabilities of false prediction and miss prediction, respectively. In false prediction, a channel is predicted as busy when it is actually free, whereas in miss prediction, a channel is predicted as free when it is actually busy. If $y_{m,l}^{\text{fp}}$ is a binary variable whose value is 1 if false prediction is occured for channel m at time slot l, and 0 otherwise. Similarly, if $y_{m,l}^{\text{mp}}$ is a binary variable whose value is 1 if miss prediction is occured for channel m at time slot l, and 0 otherwise. Then, P_{fp} and P_{mp} can be estimated empirically from the prediction history of M channels over L time slots using (14) and (15), respectively.

$$P_{\text{fp}} = \frac{\sum_{m=1}^{M}\sum_{l=1}^{L} y_{m,l}^{\text{fp}}}{LM}, \quad \forall m \in \mathcal{M},\ \forall l \in \mathcal{L} \tag{14}$$

$$P_{\text{mp}} = \frac{\sum_{m=1}^{M}\sum_{l=1}^{L} y_{m,l}^{\text{mp}}}{LM}, \quad \forall m \in \mathcal{M},\ \forall l \in \mathcal{L} \tag{15}$$

Using AF-rule, the collaborative probabilities of false prediction (Q_{fp}) and miss prediction (Q_{mp}) are derived using (16) and (17) [19], respectively.

$$Q_{\text{fp}} = \sum_{j=N-\kappa}^{N} \binom{N}{j} (P_{\text{fp}})^{j} (1 - P_{\text{fp}})^{N-j} \tag{16}$$

$$Q_{\text{mp}} = \sum_{j=N-\kappa}^{N} \binom{N}{j} (P_{\text{mp}})^{j} (1 - P_{\text{mp}})^{N-j} \tag{17}$$

C. JOINT COOPERATIVE SPECTRUM PREDICTION AND SENSING

In this phase, we combine cooperative prediction model with spectrum sensing framework in which FC performs spectrum sensing when the cooperative decision of CSP is in $\mathbb{IM}$ state, and combines the sensing results with prediction results to get a global decision about PUs existence. In a wireless fading channel environment, to attain the same level of detection probability for each of the time slots, the sensing threshold needs to be updated from one slot to another. Furthermore, with a long sensing duration, the performance of fusion results with unknown fading coefficient reaches closer to the known fading coefficient [27]. Let $\overline{P_d}$ and $\overline{P_f}$ represent the probabilities of detection and false alarm respectively of FC. Then, the required sensing time for FC to achieve target $\overline{P_d}$ and target $\overline{P_f}$ is computed by [18], [27].

$$\overline{t_s} = \frac{\left(Q^{-1}(\overline{P_f}) - Q^{-1}(\overline{P_d})\sqrt{2\gamma + 1}\right)^2}{(\gamma)^2 f_s} \tag{18}$$

where, $\overline{t_s}$ represents the required sensing time for FC. Since t_s is the maximum duration allocated for sensing in any time slot, the value of $\overline{t_s}$ should not be larger than t_s.

Let P_{H_0} and P_{H_1} denote the probabilities of a given channel to be actually idle and busy, respectively, which can be computed from channel history. Inspired from [19], the probability of a channel to be actually idle when the proposed scheme detects it as idle ($P_{0|0}$) and the probability of a channel to be actually busy but the proposed scheme detects it as idle ($P_{1|0}$) can be determined using (19) and (20), respectively.

$$P_{0|0} = \frac{P_{H_0}(1 - P_{\mathbb{IM}})(1 - Q_{\text{fp}}) + P_{H_0}P_{\mathbb{IM}}(1 - \overline{P_f})}{P_{H_0}(1 - P_{\mathbb{IM}})(1 - Q_{\text{fp}}) + P_{H_1}(1 - P_{\mathbb{IM}})Q_{\text{mp}} + P_{H_0}P_{\mathbb{IM}}} \tag{19}$$

$$P_{1|0} = \frac{P_{H_1}(1 - P_{\mathbb{IM}})Q_{\text{mp}} + P_{H_1}P_{\mathbb{IM}}(1 - \overline{P_d})}{P_{H_1}(1 - P_{\mathbb{IM}})(1 - Q_{\text{mp}}) + P_{H_0}(1 - P_{\mathbb{IM}})Q_{\text{fp}} + P_{H_1}P_{\mathbb{IM}}} \tag{20}$$

Also, using (19) and (20), we have $P_{0|1} = 1 - P_{0|0}$ and $P_{1|1} = 1 - P_{1|0}$, where, $P_{0|1}$ and $P_{1|1}$ indicate the probabilities of detecting idle channel as busy and busy channel as busy, respectively.

Using the above probabilities, the spectral efficiency and energy efficiency for the proposed scheme can be determined. Spectral efficiency for the proposed scheme is measured in terms of both improvement in average data transfer per slot by SUs and minimization of average loss of spectrum opportunity. Using (19), average data transfer per slot denoted by $\mathbb{C}$ is determined by (21).

$$\mathbb{C} = P_{0|0}\left(1 - \left(\frac{t_p}{T} + \frac{t_s}{T}\right)\right)r \tag{21}$$

where, r indicates the data rate of the channel. Similarly, loss of spectrum opportunity denoted by Φ is given by (22).

$$\Phi = 1 - P_{0|0} \tag{22}$$

Since, reduction of energy consumption plays a key role to attain energy efficiency, we compute the energy efficiency for the proposed scheme in terms of average amount of energy consumed during sensing, ratio of average data transfer per slot to the average sensing energy consumption, and ratio of average data transfer per slot to the average transmission energy consumption. The amount of energy spent during sensing denoted by $\mathbb{E}_s$ is computed using (23).

$$\mathbb{E}_s = P_{\mathbb{IM}} e_s, \tag{23}$$

where, e_s be the slot wise energy spent by FC during sensing. Again, using (21) and (23), the ratio of average data transfer per slot to the sensing energy consumption is given by (24).

$$\eta_s = \frac{\mathbb{C}}{\mathbb{E}_s} \quad , \tag{24}$$

where, η denotes the ratio of average data transfer per slot to the average sensing energy consumption.

Similarly, the amount of energy spent during transmission denoted by $\mathbb{E}_t$ is computed using (25).

$$\mathbb{E}_t = (P_{0|0} + P_{1|0})e_t, \tag{25}$$

where, e_t denotes the amount of energy spent per bit of transmission. Further, using (21) and (25), the ratio of average data transfer per slot to the transmission energy consumption is given by (26).

$$\eta_t = \frac{\mathbb{C}}{\mathbb{E}_t}, \tag{26}$$

The main steps of the proposed scheme are given in Algorithm 1.

Algorithm 1 Cooperative Spectrum Prediction-Driven Sensing

Input: Spectrum sensing history
Output: Final decision about channel status

Step 1: Local spectrum prediction:
- 1.1 Setup the LSTM network (*LN*) with input layers, LSTM layers and output layers
- 1.2 **for** ξ **do**
- 1.3 Train *LN* using training data
- 1.4 **end for**
- 1.5 Test *LN* using testing data
- 1.6 Calculate the MSE
- 1.7 If the desired accuracy is achieved in terms of MSE goto step 1.8, otherwise **repeat** step 1.3 to 1.6 with different setting of the network
- 1.8 SUs perform spectrum prediction and send local prediction results to FC for cooperation

Step 2: Cooperative spectrum prediction:
- 2.1: FC receives local prediction results from SUs
- 2.2: Perform cooperation using parallel fusion framework
- 2.3: If the cooperation model results into $\mathbb{IM}$ state then goto step 3, otherwise final decision about the channel status can be made solely based on the cooperative prediction results

Step 3: Joint cooperative spectrum prediction and sensing:
- 3.1: FC performs spectrum sensing using ED
- 3.2: Combines the sensing results with prediction results to get a final decision about channel status.

Computational Complexity: The overall computational complexity of the proposed scheme aggregates the computational complexity of each of the three main steps involves in the scheme. The computational complexity in step 1 mainly includes learning complexity of the LSTM network. During learning of LSTM network, in forward pass weighted sum of inputs from previous layer to the next are calculated whereas in backward pass errors are calculated and accordingly weights are modified. Since, the computational complexity of learning LSTM models per weight and time step with the stochastic gradient descent optimization technique is $O(1)$ [33], the overall computational complexity of the LSTM based LSP model after training of ξ epochs is $O(\xi W)$, where W indicates the total number of edges in the LSTM network. For LSTM network W is represented as $W = 4\Phi_i\Phi_h + 4\Phi_h^2 + 3\Phi_H + \Phi_h\Phi_o$, where Φ_i, Φ_o, and Φ_h indicate the number of inputs, the number of outputs, and the number of cells in the hidden layer, respectively. In step 2, the maximum number of iterations performed by FC to take a cooperative spectrum prediction decision for a channel at any time slot is N, where N indicates the number of SUs in CRN. Therefore, the computational complexity of step 2 is $O(N)$. In step 3, FC performs spectrum sensing based on cooperation prediction results, which takes a fixed amount of time. Thus, the computational complexity of step 3 is $O(K)$. Therefore, the overall computational complexity of the Algorithm 1 over a channel at any particular time slot is $O(\xi W + N + K)$.

IV. PERFORMANCE EVALUATION

A. SIMULATION SETUP

To evaluate the performance of the proposed scheme, a simulation based experiment is conducted and the results are compared with two existing schemes, namely CPM [7] and CPSS [19] from literature. In CPM scheme, a centralized CRN is considered where a SU frame is divided into three periods namely prediction period, sensing period, and transmission period. In prediction period, each of the SU performs local spectrum prediction using HMM/MLP model and sends the local prediction results to FC for cooperation. FC performs fusion of the local prediction results to get a cooperative decision using hard fusion rules. In sensing period, spectrum sensing is done to only those channels which are predicted to be available. If the spectrum sensing result is idle, the SU performs transmission in the transmission period. In CPSS scheme, all SUs perform local spectrum prediction using MLP in the prediction period of the time slot and sends their results to FC. FC combines the local prediction results to obtain a cooperative decision. After the spectrum prediction is over, the base station performs spectrum sensing in the sensing period of the time slot. In CPSS, sensing is always performed by the base station after spectrum prediction, to enhance the detection accuracy.

The performance of the proposed scheme is evaluated in terms of spectral efficiency and energy efficiency. The dataset from [25], collected by RWTH Aachen University are used. We prepare the time series data for LSP, which are divided into training dataset and testing dataset in 3:1 ratio. The training and testing of prediction model is carried out using Keras library in python. For the LSTM based local spectrum prediction model, we consider number of neurons per hidden layer as 10, number of hidden layers as 1, and learning rate equals to 0.001, respectively. We further set the length of

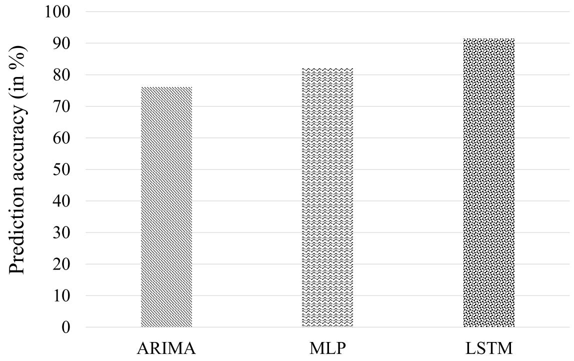

FIGURE 5. **Prediction accuracy of time-series prediction models like ARIMA, MLP, and LSTM for the dataset [25].**

time slot $T = 1000$ ms and sensing time $t_s = 100$ ms [34], prediction time $t_p = 1$ ms, energy spent per sensing $e_s = 100$ mJ, transmission energy per bit $e_t = 1$mJ, rate of channel $r = 2$ Mbps, and $P_{\alpha_e} = 9.75\%$. We run simulations for 10000 runs to compute the average result. The average result of data transfer per slot, loss of spectrum opportunity and energy spent during spectrum sensing are obtained with a 95% confidence interval that is not greater than 4.2% of the reported average results. For simulation, we introduce errors in the time series data. The errors in the binary time series are taken up to 40%, which are introduced by flipping the binary values. Maximum level of errors is considered up to 40%, because error level at 50% or above, majority of binary series data become erroneous and performance of cooperative prediction will deteriorate drastically.

B. PERFORMANCE OF THE TIME SERIES PREDICTION MODELS

To establish the efficacy of the LSTM based time series prediction model over traditional model such as MLP and auto regressive integrated moving average (ARIMA) based model, we plot a graph in Fig. 5.

Figure 5 shows the relative prediction performance of the three different time series prediction models viz. ARIMA, MLP, and LSTM. Out of the given three models, LSTM based prediction model outperforms ARIMA and MLP with approximately 15% and 9% better in prediction accuracy, respectively.

C. PERFORMANCE OF THE AF-RULE AND MAJORITY-RULE BASED COOPERATIVE PREDICTION

To show the advantage of the presented AF-rule for decision fusion over conventional majority-rule, we plot the performance of the AF-rule and Majority-rule based cooperative prediction models in Fig. 6. Figure 6 indicates that with the presence of higher error levels in time series data, prediction accuracy has deteriorated for both AF-rule and Majority-rule based cooperative prediction. However, at error levels varying from 30% to 50%, AF-rule shows an average of 8% better prediction accuracy compared to the Majority-rule. This happens due to fact that in the Majority rule, the value of

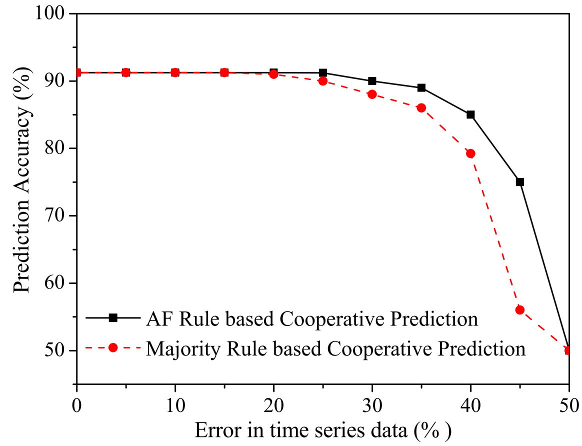

FIGURE 6. **Prediction accuracy versus errors in time series data.**

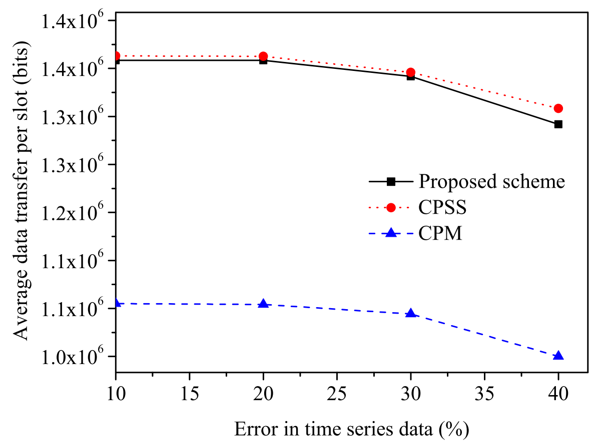

FIGURE 7. **Average data transfer per slot versus errors in time series data.**

κ in κ-out-of-N fusion rule is fixed which is equal to $\left(\frac{N}{2} + 1\right)$ whereas in AF-rule, κ is decided dynamically on the basis of error levels present in the time series data using (11).

D. SPECTRAL EFFICIENCY

We present the performance in terms of average data transfer per slot and average loss of spectrum opportunity to evaluate the spectral efficiency of the proposed scheme. Figure 7 plots the average data transfer per slot versus error level in time series data. It shows that, with increased errors in time series data, the average data transfer per slot is degraded for all three schemes. It happens due to the negative impact of errors on the performance of both local and cooperative predictions. The proposed scheme achieves 23% higher average data transfer than that of CPM when the error level is 40%, since CPM simply excludes the slots those are falsely predicted as busy and could have otherwise used. CPSS has 2% higher average data transfer per slot than that of the proposed scheme at 40% error level. This is because, in CPSS sensing is always performed after prediction, and hence has lower false prediction compared to the proposed scheme, as sensing is not performed in the proposed scheme for $\mathbb{DM}$ state.

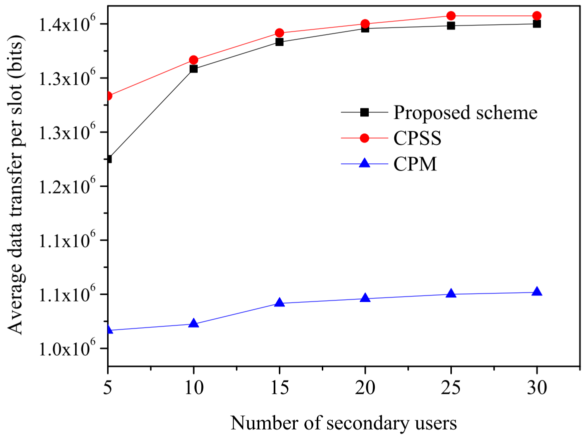

FIGURE 8. **Average data transfer per slot versus number of SUs in cooperation.**

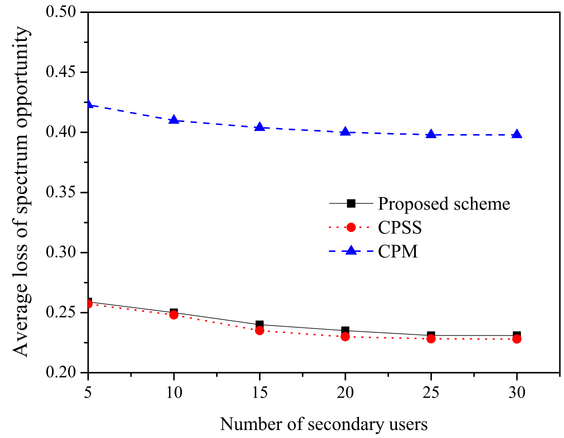

FIGURE 10. **Average loss of spectrum opportunity versus number of SUs in cooperation.**

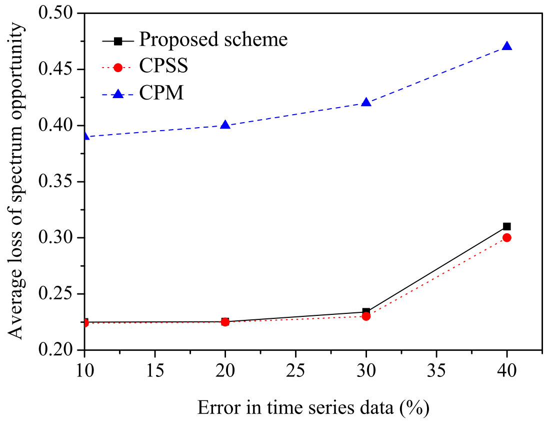

FIGURE 9. **Average loss of spectrum opportunity versus errors in time series data.**

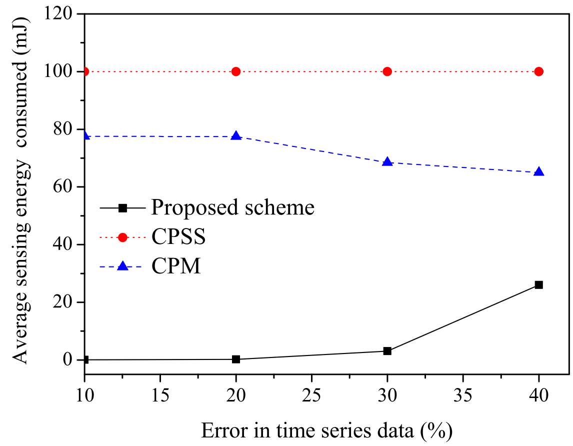

FIGURE 11. **Average amount of energy consumed during sensing versus error in time series data.**

Figure 8 reveals that increasing the SUs in cooperation increases the average data transfer for all the three schemes. This is because, more number of SUs in cooperation offsets local prediction errors of individual SU, which improves the cooperative prediction accuracy. The proposed scheme outperforms CPM because in CPM sensing is performed for only the channels those are predicted to be available, which eventually reduces the chances of exploration of falsely predicted busy channels. However, due to the always sensing policy in CPSS, the performance of CPSS is higher than the proposed scheme where sensing is performed when cooperative prediction results an $\mathbb{IM}$ state.

In Fig. 9 and Fig. 10, average loss of spectrum opportunity are plotted with respect to error and number of SUs, respectively. Figure 9 indicates that with the increase in error level in time series data, the average loss of spectrum opportunity increases for all the three schemes viz. the proposed scheme, CPM, and CPSS. This increased in spectrum opportunity loss decreases the spectral efficiency by reducing the chances of utilizing the idle slots of PU channel. But, the Fig. 9 also reflects that the proposed scheme performs around 40% better than CPM and 2% lower than CPSS in terms of average loss of spectrum opportunity when the error in time series data ranges from 10% to 40%. Figure 10 plots the average loss of spectrum opportunity with respect to varying number of SUs in cooperation. From the figure, it can be observed that with the increasing number of SUs in cooperation the loss of spectrum opportunity reduces gradually for all these three schemes. However, the proposed scheme outperforms CPM with 41% lower average spectrum opportunity loss and shows an equivalent performance with CPSS when the number of SUs ranges from 5 to 30 in cooperation.

E. ENERGY EFFICIENCY

We evaluate the energy efficiency of the proposed scheme with two different metrics: (i) average amount of energy consumed during sensing and (ii) ratio of average data transfer per slot to the average sensing energy consumption.

In Fig. 11 and Fig. 12, we demonstrates the performance of the proposed scheme in terms of average amount of energy consumed during sensing with respect to error in time series data and the number of SUs in cooperation, respectively. Figure 11 reveals that the proposed scheme consumes lesser energy in sensing operations at varying level of errors in time series data and outperforms both CPM and CPSS. The

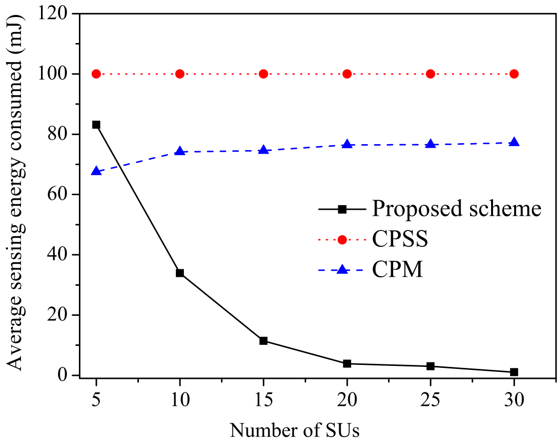

FIGURE 12. Average amount of energy consumed during sensing versus number of SUs in cooperation.

proposed scheme consumes approximately 3.8 times and 2.5 times lower sensing energy compared to CPSS and CPM, respectively, when error level reaches to 40%. The proposed scheme performs sensing only when cooperative prediction outputs an $\mathbb{IM}$ state. With the increase in errors level, the frequency of occurrences of $\mathbb{IM}$ state gets increased, leading to higher energy consumption. In contrast, energy consumption in CPM and CPSS is higher compared to the proposed scheme and follows different trends. In CPM, increase in error level escalates the false prediction, which yields a lower amount of sensing operations whereas energy consumption in CPSS is independent of level of errors and sensing is always performed irrespective of the prediction results.

Figure 12 shows that, with increase in the number of SUs in cooperation, the proposed scheme reduces energy overhead and consumes at least 33 and 25 times lower sensing energy compared to CPSS and CPM, respectively, when the number of SUs reaches up to 25 or above. In the proposed scheme, $P_{\mathbb{IM}}$ decreases with increasing SUs, which leads to reduced sensing operations, and hence lower energy consumption. Energy consumption in CPM remains at a higher level and marginally increases with increasing SUs. The positive impact of the number of SUs on prediction accuracy in CPM leads to more sensing operations with more correctly predicted idle slots. For CPSS, sensing is always performed by FC irrespective of the prediction results, and hence energy consumption remains almost constant, which is significantly higher compared to the proposed scheme.

In TABLE 1 and TABLE 2, we present the performance of the proposed scheme in terms of ratio of average data transfer per slot to the average sensing energy consumption with respect to varying level of errors in time series data and the number of SUs in cooperation, respectively. The performance in terms of above ratio provides a better insight of the proposed scheme regarding its efficacy in realistic scenario of deployment. The proposed scheme achieves approximately 3.2 times and 3.7 times better performance compared to the CPM and CPSS, respectively, when error level in time series data reaches to 40%. This is because, the proposed scheme

TABLE 1. Ratio of average data transfer per slot to the average sensing energy consumption versus error in time series data.

Error in time series data (in %)	Ratio of average data transfer per slot to the average sensing energy consumption (bits/sec/mJ)		
	CPM	CPSS	Proposed scheme
10	1.4E4	1.39E4	3.47E7
20	1.4E4	1.39E4	6.52E6
30	1.56E4	1.37E4	4.41E5
40	1.57E4	1.33E4	5.03E4

TABLE 2. Ratio of average data transfer per slot to the average sensing energy consumption versus number of SUs.

Number of secondary users	Ratio of average data transfer per slot to the average sensing energy consumption (bits/sec/mJ)		
	CPM	CPSS	Proposed scheme
5	1.53E4	1.30E4	1.47E4
10	1.41E4	1.34E4	3.91E4
15	1.43E4	1.37E4	1.18E5
20	1.40E4	1.38E4	3.58E5
25	1.41E4	1.39E4	4.57E5
30	1.40E4	1.39E4	1.32E6

TABLE 3. Ratio of average data transfer per slot to the transmission energy consumption versus error in time series data.

Error in time series data (in %)	Ratio of average data transfer per slot to the average transmission energy consumption (bits/sec/mJ)		
	CPM	CPSS	Proposed scheme
10	1.20E6	1.76E6	1.76E6
20	1.19E6	1.74E6	1.74E6
30	1.02E6	1.72E6	1.68E6
40	9.51E5	1.70E6	1.65E6

simultaneously considers the enhancement of spectral efficiency by improving detection performance and reduction of energy consumption by lowering the frequency of sensing. TABLE 2 reveals that the proposed scheme achieves 26 times and 28 times better performances than that of CPM and CPSS, respectively, when the number of SUs in cooperation ranges from 5 to 30.

In TABLE 3 and TABLE 4, we present the performance of the proposed scheme in terms of ratio of average data transfer per slot to the transmission energy consumption with respect to varying level of errors in time series data and the number of SUs in cooperation, respectively. The proposed scheme achieves approximately 1.73 times better performance compared to the CPM when error level in time series

TABLE 4. Ratio of average data transfer per slot to the transmission energy consumption versus number of SUs.

Number of secondary users	Ratio of average data transfer per slot to the transmission energy consumption (bits/sec/mJ)		
	CPM	CPSS	Proposed scheme
5	9.33E5	1.70E6	1.69E6
10	9.61E5	1.71E6	1.70E6
15	9.93E5	1.72E6	1.71E6
20	1.09E6	1.74E6	1.73E6
25	1.10E6	1.74E6	1.73E6
30	1.10E6	1.74E6	1.73E6

data reaches to 40%. This is because, the proposed scheme effectively detects the available slots using prediction-driven sensing technique, which enhances the spectral efficiency. Further, the proposed scheme achieves 97% similar performance compared to the CPSS when error level in time series data reaches to 40%. CPSS adopts an always sensing policy after prediction which results in better detection accuracy and leads to higher spectral efficiency but at the cost of higher energy overhead. TABLE 4 reveals that the proposed scheme achieves 1.57 times better performance than that of CPM and achieves similar performance compared to the CPSS, when the number of SUs in cooperation reaches to 30.

V. CONCLUSION

In this article, we proposed a cooperative spectrum prediction-driven sensing scheme to reduce energy consumption while maintaining the spectral efficiency for energy constraint CR networks. We applied an LSTM based local spectrum prediction model to identify the status of a channel before actual sensing to improve energy efficiency. We further designed a parallel fusion based centralized cooperative prediction model, which uses adaptive fusion rule to improve the performance of local prediction. Finally, the resultant cooperative prediction model was combined with a spectrum sensing framework. Sensing operation was performed only when the cooperative spectrum prediction results in an indeterminate state in order to enhance the spectral efficiency. Simulation results demonstrated that the proposed scheme outperformed both CPM and CPSS in terms of energy efficiency. It also revealed that the spectral efficiency of the proposed scheme was better than CPM and comparable to CPSS.

REFERENCES

[1] M. T. Forecasts, "Forecasts 2010-2020," in *UMTS Forum*. 2011.

[2] F. C. Commission, "Spectrum policy task force report," Tech. Rep. ET Docket 02-135, 2002.

[3] S. Haykin, "Cognitive radio: Brain-empowered wireless communications," *IEEE J. Sel. Areas Commun.*, vol. 23, no. 2, pp. 201–220, Feb. 2005.

[4] S. Maleki, S. P. Chepuri, and G. Leus, "Optimization of hard fusion based spectrum sensing for energy-constrained cognitive radio networks," *Phys. Commun.*, vol. 9, pp. 193–198, Dec. 2013.

[5] K. Kulkarni and A. Banerjee, "Multi-channel sensing and resource allocation in energy constrained cognitive radio networks," *Phys. Commun.*, vol. 23, pp. 12–19, Jun. 2017.

[6] F. Hu, B. Chen, and K. Zhu, "Full spectrum sharing in cognitive radio networks toward 5G: A survey," *IEEE Access*, vol. 6, pp. 15754–15776, 2018.

[7] N. Shaghluf and T. A. Gulliver, "Spectrum and energy efficiency of cooperative spectrum prediction in cognitive radio networks," *Wireless Netw.*, vol. 25, pp. 1–10, Mar. 2018.

[8] V. K. Tumuluru, P. Wang, and D. Niyato, "A neural network based spectrum prediction scheme for cognitive radio," in *Proc. IEEE Int. Conf. Commun.*, May 2010, pp. 1–5.

[9] Z. Chen, N. Guo, Z. Hu, and R. C. Qiu, "Experimental validation of channel state prediction considering delays in practical cognitive radio," *IEEE Trans. Veh. Technol.*, vol. 60, no. 4, pp. 1314–1325, May 2011.

[10] A. Saad, B. Staehle, and R. Knorr, "Spectrum prediction using hidden Markov models for industrial cognitive radio," in *Proc. IEEE 12th Int. Conf. Wireless Mobile Comput., Netw. Commun. (WiMob)*, Oct. 2016, pp. 1–7.

[11] Z. Jin, K. Yao, B. Lee, J. Cho, and L. Zhang, "Channel status learning for cooperative spectrum sensing in energy-restricted cognitive radio networks," *IEEE Access*, vol. 7, pp. 64946–64954, 2019.

[12] A. H. Chowdhury, Y. Song, and C. Pang, "Accessing the hidden available spectrum in cognitive radio networks under GSM-based primary networks," in *Proc. IEEE Int. Conf. Commun. (ICC)*, May 2017, pp. 1–6.

[13] J. Yang, H.-S. Zhao, X. Chen, J.-Y. Xu, and J.-Z. Zhang, "Energy-efficient design of spectrum prediction in cognitive radio networks: Prediction strategy and communication environment," in *Proc. 12th Int. Conf. Signal Process. (ICSP)*, Oct. 2014, pp. 154–158.

[14] J. Sun, J. Wang, G. Ding, L. Shen, J. Yang, Q. Wu, and L. Yu, "Long-term spectrum state prediction: An image inference perspective," *IEEE Access*, vol. 6, pp. 43489–43498, 2018.

[15] C. Ge, Z. Wang, and X. Zhang, "Robust long-term spectrum prediction with missing values and sparse anomalies," *IEEE Access*, vol. 7, pp. 16655–16664, 2019.

[16] F. Zhou, G. Lu, M. Wen, Y.-C. Liang, Z. Chu, and Y. Wang, "Dynamic spectrum management via machine learning: State of the art, taxonomy, challenges, and open research issues," *IEEE Netw.*, vol. 33, no. 4, pp. 54–62, Jul. 2019.

[17] S. D. Barnes, B. T. Maharaj, and A. S. Alfa, "Cooperative prediction for cognitive radio networks," *Wireless Pers. Commun.*, vol. 89, no. 4, pp. 1177–1202, 2016.

[18] H. Eltom, S. Kandeepan, Y. Chang Liang, B. Moran, and R. J. Evans, "HMM based cooperative spectrum occupancy prediction using hard fusion," in *Proc. IEEE Int. Conf. Commun. Workshops (ICC)*, May 2016, pp. 669–675.

[19] V.-D. Nguyen and O.-S. Shin, "Cooperative prediction-and-sensing-based spectrum sharing in cognitive radio networks," *IEEE Trans. Cognit. Commun. Netw.*, vol. 4, no. 1, pp. 108–120, Mar. 2018.

[20] I. F. Akyildiz, B. F. Lo, and R. Balakrishnan, "Cooperative spectrum sensing in cognitive radio networks: A survey," *Phys. Commun.*, vol. 4, no. 1, pp. 40–62, Mar. 2011.

[21] L. Yu, J. Chen, G. Ding, Y. Tu, J. Yang, and J. Sun, "Spectrum prediction based on taguchi method in deep learning with long short-term memory," *IEEE Access*, vol. 6, pp. 45923–45933, 2018.

[22] H. Urkowitz, "Energy detection of unknown deterministic signals," *Proc. IEEE*, vol. 55, no. 4, pp. 523–531, Apr. 1967.

[23] J. Gupta, P. Chauhan, M. Nath, M. Manvithasree, S. K. Deka, and N. Sarma, "Coalitional game theory based cooperative spectrum sensing in CRNs," in *Proc. 18th Int. Conf. Distrib. Comput. Netw.*, Jan. 2017, pp. 1–7.

[24] S. K. Deka, P. Chauhan, and N. Sarma, "Constraint based cooperative spectrum sensing for cognitive radio network," in *Proc. Int. Conf. Inf. Technol.*, Dec. 2014, pp. 63–68.

[25] M. Wellens, J. Riihijärvi, and P. Mähönen, "Empirical time and frequency domain models of spectrum use," *Phys. Commun.*, vol. 2, nos. 1–2, pp. 10–32, Mar. 2009.

[26] X. Hao, M. H. Cheung, V. W. S. Wong, and V. C. M. Leung, "A coalition formation game for energy-efficient cooperative spectrum sensing in cognitive radio networks with multiple channels," in *Proc. IEEE Global Telecommun. Conf. (GLOBECOM)*, Dec. 2011, pp. 1–6.

[27] Y.-C. Liang, Y. Zeng, E. C. Y. Peh, and A. T. Hoang, "Sensing-throughput tradeoff for cognitive radio networks," *IEEE Trans. Wireless Commun.*, vol. 7, no. 4, pp. 1326–1337, Apr. 2008.

[28] G. Chen, "A gentle tutorial of recurrent neural network with error backpropagation," 2016, *arXiv:1610.02583*. [Online]. Available: http://arxiv.org/abs/1610.02583

[29] S. Varma and R. Simon, "Bias in error estimation when using cross-validation for model selection," *BioMed Central*, vol. 7, no. 1, p. 91, 2006.

[30] A. S. B. Kozal, M. Merabti, and F. Bouhafs, "An improved energy detection scheme for cognitive radio networks in low SNR region," in *Proc. IEEE Symp. Comput. Commun. (ISCC)*, Jul. 2012, pp. 684–689.

[31] R. Viswanathan and P. K. Varshney, "Distributed detection with multiple sensors I. Fundamentals," *Proc. IEEE*, vol. 85, no. 1, pp. 54–63, Jan. 1997.

[32] W. Saad, Z. Han, M. Debbah, A. Hjorungnes, and T. Basar, "Coalitional games for distributed collaborative spectrum sensing in cognitive radio networks," in *Proc. IEEE 28th Conf. Comput. Commun. (INFOCOM)*, Apr. 2009, pp. 2114–2122.

[33] H. Sak, A. Senior, and F. Beaufays, "Long short-term memory recurrent neural network architectures for large scale acoustic modeling," in *Proc. 15th Annu. Conf. Int. Speech Commun. Assoc.*, 2014, pp. 1–5.

[34] A. El Shafie, M. Ashour, A. Mohamed, and T. Khattab, "Optimal spectrum access for a rechargeable cognitive radio user based on energy buffer state," in *Proc. Int. Conf. Comput., Netw. Commun. (ICNC)*, Feb. 2015, pp. 242–247.

PRAKASH CHAUHAN received the M.C.A. degree from the Department of Computer Science and Engineering, Tezpur University, India, in 2014, where he is currently pursuing the Ph.D. degree. His research interests include spectrum sensing and resource allocation in cognitive radio networks. He has served as a Reviewer for IEEE TRANSACTIONS ON VEHICULAR TECHNOLOGY, IEEE ACCESS, and *Wireless Network* (Springer).

SANJIB K. DEKA (Member, IEEE) received the B.E. degree in computer science and engineering from Dibrugarh University, in 1998, and the M.Tech. degree in information technology and the Ph.D. degree in computer science and engineering from Tezpur University, India, in 2000 and 2016, respectively. He has worked with Sasken Communication Technologies Ltd., Bengaluru, India, and Cisco Systems India Pvt., Ltd., Bengaluru. He is currently working as an Associate Professor with the Department of Computer Science and Engineering, Tezpur University. He has published more than 20 papers in international journals/conference proceedings. His research interests include cognitive radio networks, resource allocation, and scheduling problems for wireless networks. He is a Lifetime Member of IETE. He has served as a Reviewer for IEEE TRANSACTIONS ON NETWORK SCIENCE AND ENGINEERING, IEEE TRANSACTIONS ON COGNITIVE COMMUNICATIONS AND NETWORKING, IEEE ACCESS, and *IET Networks*.

BIJOY CHAND CHATTERJEE (Senior Member, IEEE) received the Ph.D. degree from the Department of Computer Science and Engineering, Tezpur University, in 2014. He is currently an Assistant Professor and a DST Inspire Faculty with South Asian University (SAU), New Delhi, India. Before joining at SAU, he was with IIITD, India, the Norwegian University of Science and Technology, Trondheim, Norway, and The University of Electro-Communications, Tokyo, Japan. His research interests include optical networks, QoS-aware protocols, optimization, and routing. He is a professional Life Member of IETE. He was a recipient of several prestigious awards, including the IETE Research Fellowship from the Institution of Electronics and Telecommunication Engineers, India, in 2011, the UEC Postdoctoral Research Fellowship from The University of Electro-Communications, in 2014, the ERCIM Postdoctoral Research Fellowship from the European Research Consortium for Informatics and Mathematics, in 2016, and the DST Inspire Faculty Award in 2017.

NITYANANDA SARMA (Member, IEEE) received the B.E. degree from the Jorhat Engineering College, Jorhat, under Dibrugarh University, in 1991, the M.Tech. degree from IIT Kharagpur, and the Ph.D. degree from IIT Guwahati, all in computer science and engineering. He is currently working as a Professor with the Department of Computer Science and Engineering, Tezpur University, India. Before joining Tezpur University, he was a Faculty Member with the Department of Computer Science and Engineering, Jorhat Engineering College, till 1999. He has also served as a Guest Lecturer with the North Eastern Regional Institute of Science and Technology, from January 1992 to May 1992. In 1999, he joined Tezpur University, where he is currently a Professor with the Department of Computer Science and Engineering. He has published more than 110 papers in international/national journals and conference proceedings, one book, and two edited volumes. His research interests include ad hoc networks, QoS supports in wireless networks, channel assignment in cognitive radio networks, and WDM optical networks. He is a Professional Member of IEEE and ACM and a Fellow of IETE.